Molekul, Vol. 20. No. 2, July 2025: 382 – 393

MOLEKUL
eISSN: 2503-0310

Articles

https://doi.org/10.20884/1.jm.2025.20.2.16066

Chemical Constituents from Indonesian *Dysoxylum parasiticum* (Osbeck). Kosterm and Their Cytotoxicity Against MCF-7 Breast Cancer Cells

Harizon[1]*, Febbry Romundza, Isra Miharti, Al Arofatus Naini[2], Sofa Fajriah[2], Tri Mayanti[3], Unang Supratman[3,4]

[1]Faculty of Teacher Training and Education, Universitas Jambi, Mendalo Indah, Jambi 36361, Indonesia
[2]Research Center for Pharmaceutical Ingredients and Traditional Medicine, National Research and Innovation Agency (BRIN), Cibinong Science Center Complex – BRIN, Cibinong 16911, Bogor, West Java, Indonesia
[3]Department of Chemistry, Faculty of Mathematics and Natural Sciences, Universitas Padjadjaran, Jatinangor 45363, Sumedang, West Java, Indonesia
[4]Central Laboratory, Universitas Padjadjaran, Jatinangor 45363, Sumedang, West Java, Indonesia

*Corresponding author email: harizon@unja.ac.id

Received June 12, 2025; **Accepted** July 17, 2025; **Available online** July 20, 2025

ABSTRACT. The exploration of naturally occurring secondary metabolites from plants, which serve as direct sources or precursors for new drug development, motivates us to conduct a comprehensive investigation into their presence. Indonesia stands out as a global biodiversity hotspot, boasting a significant number of endemic species that offer a rich reservoir of untapped resources for pharmaceutical, agricultural, and environmental uses. The *Dysoxylum* genus, belonging to the Meliaceae family, is recognized as a vital source of secondary metabolites and is well-known for its traditional medicinal applications. Consequently, we focus on analyzing the chemical constituents found in the stem bark of one Indonesian *Dysoxylum* species, specifically *D. parasiticum* (Osbeck) Kosterm., and assess their biological activity as anticytotoxic agents. Our research identified three known compounds: a tirucallane-type triterpenoid, cneorin-NP$_{36}$ (**1**), a *seco*-limonoid from the preurianin group, amotsangin A (**2**), and an ergostane-type steroid, 22(*E*)-ergosta-6,22-dien-3*β*,5*α*,8*α*-triol (**3**). The biological evaluation against the human breast cancer cell line MCF-7 revealed that compound **2** exhibited a notable inhibitory effect, with an IC$_{50}$ value of 34.5 µM. The existence of a highly oxidized structure in compound **2**, due to its ester substituents, highlights its effectiveness in inhibiting cancer cell proliferation, outperforming the reference drug cisplatin, which has an IC$_{50}$ of 53.0 µM. These findings indicate that amotsangin A (**2**) is a promising anticancer agent, particularly in the treatment of breast cancer. Further studies, including *in silico* analysis and structural modification, are needed to enhance its cytotoxic activity and selectivity.

Keywords: Cytotoxic activity, *Dysoxylum parasiticum*, MCF-7, *seco*-limonoid amotsangin A, Secondary metabolites

INTRODUCTION

The *Dysoxylum* genus serves as a significant source of secondary metabolites. Part of the Meliaceae family, this genus includes around 200 species predominantly located in Australia, New Zealand, India, and Southeast Asia (Lakshmi et al., 2009; Naini et al., 2022b; Xu et al., 2013; Huang, et al., 2011; Wang & Guan, 2012; Hu et al., 2014; Yan et al., 2021). The Meliaceae, commonly referred to as Mahogany, consists of plants characterized by their woody structure, making this family renowned for its production of high-quality timber (Atkinson, 2020). Additionally, this family is noted for its wood, which emits a distinctive aroma (Riyadi et al., 2023; Tan et al., 2011; Naini et al., 2022a; Naini et al., 2023a). Historically, these plants have been employed as traditional remedies by indigenous populations in Asia to treat various ailments, such as *D. binectariferum* and *D. lourieri* for skin conditions and ulcers (Hu et al., 2014; Yan et al., 2021; Kumar at al., 2016; Sarkar & Devi, 2017; Ashwell & Walston, 2008; Chanda et al., 2007; Bourdy et al., 1996), *D. gaudichaudianum* leaves for a range of pains and respiratory issues (Sarkar & Devi, 2017; Ashwell & Walston, 2008; Chanda et al., 2007; Nagakura., 2010; Jian et al., 2007; Lalmuanpuii et al., 2013), and *D. richii* for joint stiffness and skin irritations (Ashwell & Walston, 2008; Chanda et al., 2007; Bourdy et al., 1996; Jogia & Andersen, 1987; Singh & Aalbersberg, 1992). In Indonesia, numerous species have been identified and cultivated, many of which yield novel compounds, including triterpenoids, limonoids, steroids, and macrolides, and some exhibiting moderate activity against human cancer cells (Naini et al., 2022a; Niani et al., 2023a; Naini et al., 2023b; Riyadi et al., 2024a; Riyadi et al., 2024c; Kautsari et al., 2024a; Naini et al., 2024b).

Dysoxylum parasiticum (Osbeck) Kosterm. (Meliaceae) is a large tree species that can reach heights up to 38 meters and is commonly known as the aromatic tree or "Majegau". This species is extensively cultivated, especially in West Java and Bali, and holds cultural significance for various indigenous ethnic groups. Phytochemical investigations of this plant have uncovered a substantial presence of terpenoids, which show immunomodulatory effects on TLR4 and possess cytotoxic properties. Key compounds identified include sesquiterpenoids and their oligomers (Naini et al., 2023a; Naini et al., 2023b; Naini et al., 2024b;), triterpenoids (Naini et al., 2022a), limonoids (Naini et al., 2024a), and phenolic derivatives (Sofian et al., 2022). As part of our ongoing research into bioactive secondary metabolites, we examined the chemical constituents of the stem barks of *D. parasiticum*. This study identified three known compounds: a tirucallane-type triterpenoid, cneorin-NP36 (**1**), a *seco*-limonoid from the preurianin group, amotsangin A (**2**), and an ergostane-type steroid, 22(*E*)-ergosta-6,22-dien-3*β*,5*α*,8*α*-triol (**3**). The structures of the compounds were elucidated using high-resolution mass spectrometry (HRMS), infrared spectroscopy (IR), one-dimensional (1D) and two-dimensional (2D) nuclear magnetic resonance (NMR), along with comparisons to previously reported data.

EXPERIMENTAL

General Experimental Procedures

NMR data were acquired using JEOL ECZR 500 NMR (JEOL USA, Inc., USA) spectrometer. High-resolution mass spectrometry (HR-MS) was performed with a Waters Xevo Quadrupole-TOF-MS/direct probe (Milford, MA), operating in ESI+ mode. Infrared spectra were recorded using Everest ATR Thermo Scientific (Thermo Fisher Scientific, Madison, WI, USA). The melting point values were determined using a BUCHI M-565 melting point apparatus (BUCHI Corp., Switzerland). For column chromatography (CC), silica gel (230–400 and 70-230 mesh) and Octadecyl silane (100-200 mesh) were sourced from Merck (Germany) and Fuji Sylisia Chemical LTD. (Japan). Thin layer chromatography (TLC) was conducted using silica gel GF_{254} and RP-18 F_{254}s plates, both obtained from Merck. The TLC analysis was performed under ultraviolet light and subsequently visualized using a 10% H_2SO_4/EtOH solution, followed by a heating process.

Plant Material

The stem barks of *Dysoxylum parasiticum* (Osbeck) Kosterm (**Figure 1**). were gathered from the Bogor Botanical Garden (BBG) located in West Java Province, Indonesia. The botanical specimen underwent morphological authentication by Mr. Harto from the BBG Herbarium and was designated the voucher specimen with barcode III. F.79.

Extraction and Isolation

The dried and powdered stem bark (5.5 kg) underwent extraction with methanol (3 x 12 L) at room temperature, with each extraction period extending for 24 hours. The partitioning procedure was detailed in earlier studies, which included the initial phase of chromatographic separation of the *n*-hexane extract (153.9 g), yielding eight primary fractions labeled Fr. A to Fr. L [11,12,23,27]. Fraction D, weighing 40.9 g, underwent column chromatography using silica gel (70–230 mesh) with a gradient elution of *n*-hexane and EtOAc (10:0 to 7:3, 5% v/v), resulting in the isolation of nine additional fractions designated as Fr. D1 through Fr. D9.

(**A**) (**B**)

Figure 1. *Dysoxylum parasiticum* (Osbeck) Kosterm. (**A**) and stem barks (**B**) (Private Photograph Courtesy).

Subsequently, Fraction D7, weighing 5.0 g, was further purified using silica gel column chromatography (70–230 mesh) and eluted with a mixture of *n*-hexane and EtOAc (10:0 to 5:5, 2.5% v/v), yielding eight subfractions labeled D7a to D7h. Subfraction D7a, weighing 800 mg, was then subjected to column chromatography on silica gel (230–400 mesh), eluted with a solvent system of *n*-hexane, dichloromethane, and EtOAc (7:2:1), and subsequently refined using flash ODS reversed-phase column chromatography with a MeOH–H_2O mixture (8:2), ultimately producing compound **1** in a yield of 7.1 mg. Subfraction D7b (300 mg) was subjected to separation using silica gel (230–400 mesh) with an eluent mixture of *n*-hexane and EtOAc (10:1). The resulting product was further purified through ODS column chromatography employing a MeOH and H_2O mixture (8:2), yielding compound **3** (4.0 mg). Furthermore, fraction D9 (2.0 g) was applied to a silica gel column (230–400 mesh) and eluted using a mixture of CH_2Cl_2 and EtOAc (10:0 to 5:5, 10% v/v), resulting in the separation of six subfractions designated as D9a through D9f. Subfraction D9d (300 mg) underwent purification via flash ODS column chromatography using a MeOH–H_2O solvent system (8:2), yielding compound **2** (15.1 mg).

Cytotoxic Assay

A cytotoxicity assay was conducted following established protocols (Kautsari et al., 2024b; Riyadi et al., 2024b). The isolated compounds (**1–3**) were assessed for their cytotoxic effects on human breast cancer cell lines (MCF-7) utilizing RPMI-1640 medium enriched with 10% fetal bovine serum (FBS) and 1% antibiotics. After a 24-hour incubation period, cell viability was determined using Prestoblue™ reagent, with measurements taken at 570 nm using a microplate reader.

RESULTS AND DISCUSSION

The phytochemical investigation of *Dysoxylum parasiticum* (Osbeck). Kosterm stem barks isolated from *n*-hexane extract yielded one tirucallane-type triterpenoid, cneorin-NP_{36} (**1**), one preurianine-type limonoid, amotsangin A (**2**), one ergostane-type steroid, 22(*E*)-ergosta-6,22-dien-3*β*,5*α*,8*α*-triol (**3**), and one coumarin-type phenylpropanoid, scopoletin (**4**). The isolation and purification were performed by a combination of chromatography techniques between normal and reversed phases, as well as utilizing a thin layer chromatography (TLC) with universal sprayer reagent of H_2SO_4 in 10% EtOH.

Cneorin-NP_{36} (**1**), was isolated as a white crystalline material. The molecular formula was determined to be $C_{30}H_{46}O_3$, with the molecular ion peak observed in HR-ESI-QTOFMS at *m/z* 455.3596 $[M + H]^+$ (calculated for $C_{30}H_{47}O_3$, 455.3678), indicating eight degrees of unsaturation. The NMR analysis of compound **1** revealed a tetracyclic triterpenoid framework, featuring one secondary methyl group at δ_H 1.04 (3H, d, J = 6.5 Hz), seven tertiary methyl groups at δ_H 0.77; 0.99; 1.03; 1.03; 1.09; 1.32; 1.32; 1.39 ppm, and four non-oxygenated aliphatic quaternary carbons at δ_C 35.1; 43.9; 50.8; and 58.4 ppm. The HMQC analysis indicated the presence of typical double bond signals attributed to the fragment C-7/C-8 [-CH=C=] at δ_C 118.4 (δ_H 5.35, 1H, td, J = 3.5, 3.5 Hz) and 145.7 ppm, suggesting a tirucallane-type skeleton. This assignment was proved by the HMBC correlations from H_3-30 (δ_H 1.03); H-9 (δ_H 2.32); H-7 (δ_H 5.35); H-6 (δ_H 2.06 and 2.78); to C-8 (δ_C 145.7) and vicinal cross-peaks of the B-ring fragment (H-5/H-6/H-7) in the ^{1}H-^{1}H COSY spectrum. In addition to the characteristics of tirucallane skeleton with a double bond pair at C-7/C-8, the position of vicinal dimethyl group at C-13 and C-14 was further assigned based on the HMBC correlations of H_3-18 (δ_H 0.99) and H_3-30 (δ_H 1.03) to C-13 (δ_C 43.9) and C-14 (δ_C 50.8). The ketone carbonyl group at δc 216.9 ppm was also observed in **1**, where the position of the oxygenated carbon at C-3 was determined based on the biogenesis pathway of the triterpenoid compound derived from 2,3-epoxy squalene and convinced by HMBC correlations of H_3-28 (δ_H 1.09) and H_3-29 (δ_H 1.03) to C-13 (δ_C 43.9) and C-14 (δ_C 50.8). Furthermore, the HMBC correlations of H_3-19 (δ_H 0.99) to C-1 (δ_C 38.5); C-5 (δ_C 52.3); C-9 (δ_C 48.4); and C-10 (δ_C 35.1) completed the A-ring fragment in the tetracyclic system of tirucallane-type triterpenoid in compound **1**.

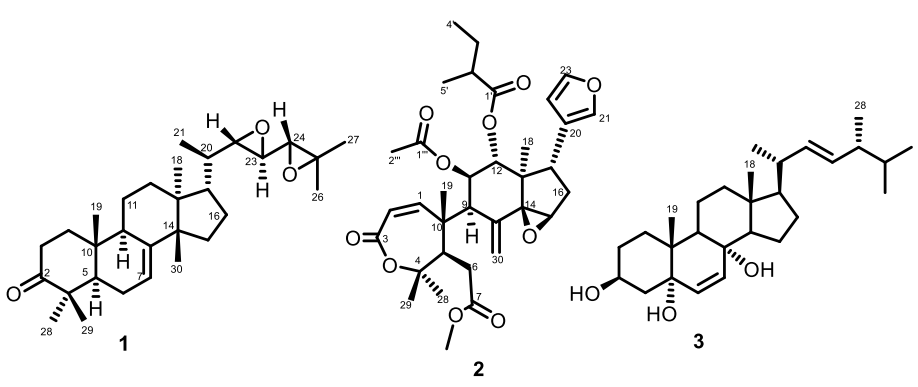

Figure 2. Structure of chemical constituents of *D. parasiticum* (Osbeck) Kosterm. stem barks **1-3.**

Analysis of the 2D NMR above implies that compound **1** had two additional cyclic to meet the value of unsaturation degrees from the MS data. The presence of four oxygenated carbons, including three methines [δ_C 60.5/C-22 (δ_H 2.60, 1H, dd, J=8.0; 2.5 Hz), 57.5/C-23 (δ_H 2.78, 1H, dd, J=6.5 1.8 Hz), 63.2/C-24 (δ_H 2.55, 1H, d, J=6.4 Hz)] and one quaternary group [δ_C 58.4/C-225], was assumed to form two epoxy rings in the side chain. The ^{1}H-^{1}H COSY correlations of coupling-coupling system from H_3-21/(H-20)/H-22/H-23/H-24 and $^3J_{H\text{-}C}$ interactions of H_3-26 (δ_H 1.39) and H_3-27 (δ_H 1.32) to C-25 (δ_C 58.4) and C-24 (δ_C 63.2) placed the two adjacent epoxy rings at C-22-*O*-C-23 and C-24-*O*-C-25, respectively. Thus, the planar structure of **1** was fully constructed based on the NMR data, as shown in **Figure 3**. As tirucallane-type triterpenoid possesses the same planar structure as its C-21 stereoisomer, i.e., euphane-type (Huang et al., 2011; Hill & Connolly, 2017; Sawai & Saito, 2011; Zhang et al., 2010; Liu et al., 2001), the stereochemistry of **1** needs to be deduced. A NOESY experiment was subsequently carried out to determine the relationship between each stereocenter carbon and its surrounding space. The NOE correlations observed between H_3-19/H_3-29, H-17/H_3-30, and H-17/H_3-21 as β-oriented protons, along with α-proton correlations of H_3-28/H-5, H-9α/H_3-18, and H_3-18/H-20, aligned with that of the tirucallane skeleton, in particular the β-orientation of the secondary methyl group at C-21 (**Figure 4**). The correlations among the proton-proton interactions of the asymmetrical carbon in the side chain can be detected in the NOESY spectrum; however, the free rotation and vicinal positioning of the two epoxy rings invalidate this information, necessitating an alternative approach. The NMR data for compound **1** were subsequently compared with the previously identified compound cneorin-NP$_{36}$, as first reported by Gray and co-workers (see **Table 1**) (Gray et al., 1988). The analysis revealed that both compounds exhibited identical chemical shifts, indicating that compound **1** possesses a planar structure with the orientations of H-22, H-23, and H-24 configured as β. In cyclic epoxide systems, *cis*-conformational vicinal protons typically exhibit coupling constant values ranging from 7 to 12.6 Hz; however, in compound **1**, the ^2J values for H-22/H-23 were measured at 8.0; 2.5 and 6.5; 1.8 Hz, respectively. Furthermore, Wang et al. provided a revised structure for cneorin-NP$_{36}$, indicating that H-23 is oriented α, with an absolute configuration of 22*S**, 23*S**, and 24*S** determined through X-ray diffraction analysis (Wang et al., 2011). Consequently, compound **1** was identified and confirmed as the corrected form of cneorin-NP$_{36}$ (**Figure 2**).

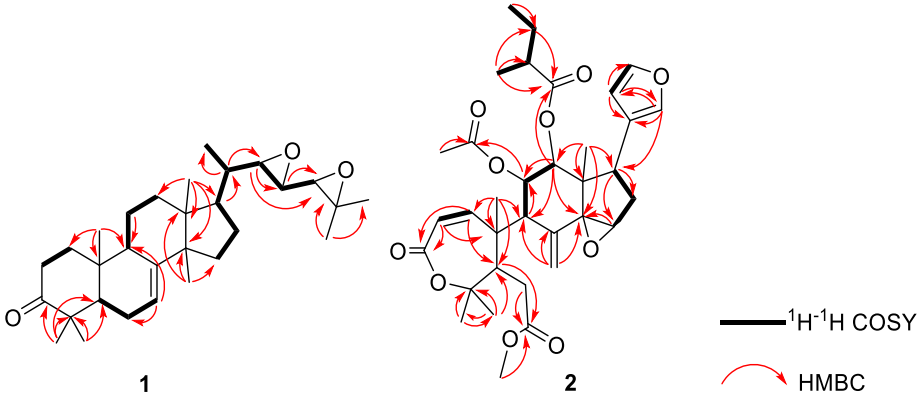

Figure 3. ^{1}H-^{1}H COSY and HMBC correlations of **1** and **2**.

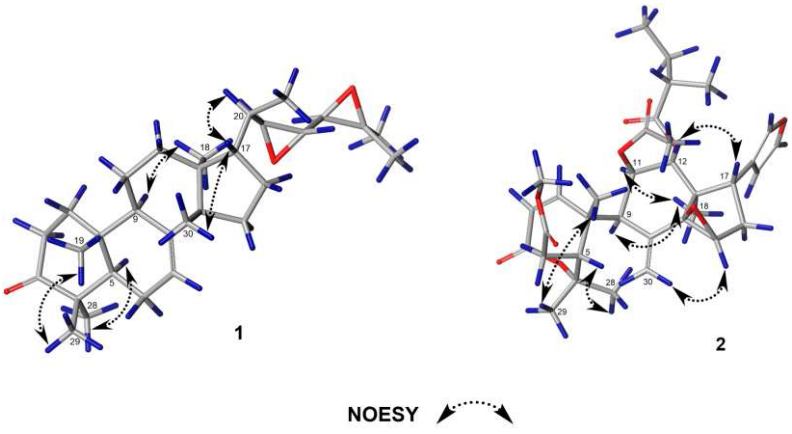

Figure 4. ^{1}H-^{1}H NOESY correlations of **1** and **2**

Table 1. NMR data (^{1}H and ^{13}C-NMR, $CDCl_3$) of **1** with literature (^{13}C-NMR, $CDCl_3$)

No.	Compound **1** ($CDCl_3$)		Cneorin-NP_{36} ($CDCl_3$). (Gray et al., 1988; Wang et al., 2011)
	^{1}H NMR (ΣH, mult., *J* Hz)	^{13}C NMR (mult.)	^{13}C NMR (mult.)
1.	1.98 (1H, *ddd*, 13.0; 5.5; 3.5) 1.46 (1H, *m*)	38.5 (t)	38.4 (t)
2.	2.23 (1H, *dt*, 14.5; 3.5) 2.78 (1H, *td*, 14.5; 5.5)	34.9 (t)	34.7 (t)
3	-	216.9 (s)	216.4 (s)
4.	-	47.9 (s)	47.7 (s)
5.	1.75 (1H, *m*)	52.3 (d)	52.2 (d)
6.	2.06 (1H, *m*) 2.25 (1H, *m*)	24.4 (t)	24.3 (t)
7.	5.35 (1H, *td*, 3.5; 3.5)	118.4 (d)	118.1 (d)
8.	-	145.7 (s)	145.3 (s)
9	2.32 (1H, *m*)	48.4 (d)	48.3 (d)
10.	-	35.1 (s)	34.9 (s)
11.	1.58 (1H, *m*)	18.2 (q)	18.0 (q)
12.	1.64 (1H, *m*) 1.85 (1H, *m*)	33.3 (t)	33.2 (t)
13.	-	43.9 (s)	43.8 (s)
14.	-	50.8 (s)	50.7 (s)
15.	1.54 (1H, *m*)	34.2 (d)	34.1 (d)
16.	1.35 (1H, *m*) 1.98 (1H, *m*)	27.5 (t)	27.3 (t)
17.	1.70 (1H, *m*)	50.5 (d)	50.4 (d)
18.	0.77 (3H, *s*)	12.8 (q)	12.6 (q)
19.	0.99 (3H, *s*)	21.6 (q)	21.4 (q)
20.	1.28 (1H, *m*)	39.1 (d)	39.0 (d)
21.	1.04 (3H, *d*. 6.5)	16.6 (q)	16.3 (q)
22.	2.60 (1H, *dd*, 8.0; 2.5)	60.5 (d)	60.3 (d)
23.	2.78 (1H, *dd*, 6.5; 1.8)	57.5 (d)	57.3 (d)
24.	2.55 (1H, *d*, 6.4)	63.2 (d)	63.2 (d)
25.	-	58.4 (s)	58.2 (s)
26.	1.39 (3H, *s*)	19.7 (q)	19.5 (q)
27.	1.32 (3H, *s*)	24.8 (q)	24.6 (q)
28.	1.09 (3H, *s*)	24.6 (q)	24.5 (q)
29.	1.03 (3H, *s*)	21.6 (q)	21.4 (q)
30.	1.03 (3H, *s*)	27.6 (q)	27.4 (q)

Amotsangin A (**2**), was isolated as an optically active white crystalline substance, exhibiting a specific rotation of $[\alpha]^{D}_{25}$ +108.5. Additionally, it displayed a bathochromic shift in its UV absorption spectrum, with absorption maxima recorded at 218 nm. High-resolution electrospray ionization mass spectrometry (HRESIMS) analysis shows the molecular formula as $C_{34}H_{44}O_{10}$ at *m/z* 635.2841 $[M + Na]^+$ (calculated for $C_{34}H_{44}O_{10}Na$, *m/z* 635.2832), manifesting 13 degrees of unsaturation. The infrared (IR) spectrum revealed the presence of various functional groups, including CH sp^3 (2978 cm^{-1}), carbonyl ester (1751 cm^{-1}), conjugated carbonyl ester (1697 cm^{-1}), C=C (1644 cm^{-1}), *gem*-dimethyl (1462, 1431 cm^{-1}) and C-O (1233 cm^{-1}. The ^{1}H NMR (Table 2) suggested a set of furan group shifts [δ_H 7.25 (1H, s), 7.07 (1H, s) and 6.17 (1H, s) ppm], one methoxy at δ_H 3.69 (3H, s) ppm, one acetyl [δ_H 2.08 (3H, s) ppm], four tertiary methyls [δ_H 1.52 (3H, s), 1.25 (3H, s), 1.52 (3H, s), 0.96 (3H, s), and 0.93 (3H, s) ppm], and one primary methyl at δ_H 0.73 (3H, t, *J* = 7.3 Hz) ppm. The ^{13}C NMR and DEPT of compound **2**, together with the HMQC spectra displayed the presence of a total of 34 carbons, including four carbonyl esters (one conjugated) [δ_C 175.0; 173.5; and 166.5 ppm], eight sp^2 carbons (one methylene, five methine and two quaternary carbons), 22 aliphatic carbons (comprising two oxygenated quaternary carbons, three oxygenated methins and one methoxy). The presence of one furan ring, three olefinic bonds and four carboxyls was calculated as nine degrees of unsaturation, so a tetracyclic skeleton is required to satisfy the

unsaturation degree values. The presence of two non-oxygenated aliphatic quaternary carbons [δ_C 46.2 (C-10) and 45.6 (C-13) ppm] and one methylene sp^2 [δ_C 120.8 (C-30) ppm] indicated the presence of a *seco* group (modified ring) with two intact rings of the limonoid compound. Analysis of $^3J_{H-C}$ correlations through an HMBC experiment indicated the presence of *seco*-A,B ring groups through the correlation of H_3-28 (δ_H 1.25)/H_3-29 (δH 1.55) to C-4 (δ_C 83.5), C-5 (δ_C 50.3) and H-30 (δ_H 5.17 and 5.34) to C-8 (δ_C 136.9), C-9 (δ_C 53.4), C-14 (δ_C δc 71.1). HMBC correlations of H_3-19 (δ_H 0.96) to C-1 (δ_C 148.5), C-10 (δ_C 46.2) coupled with H-1/H-2 correlation at ^{1}H-^{1}H COSY confirmed the α,β-unsaturated-ε-caprolactone fragments in ring A, while open ring B was evidenced from long-range interractions of -OMe (δ_H 3.66)/H-5 (δ_H 3.25) with C-7 (δ_C 173.5). The intact C,D-ring was determined based on the correlation of H_3-18 (δ_H 0.93) to C-12 (δ_C 73.6), C-13 (δ_H 43.6), C-17 (δ_H 42.7) and H-16 (δ_H 5.46)/H_3-18 (δ_H 0.93) to C-14 (δ_H 71.1), as well as the two vicinal proton segments of H-9/H-11/H-12 and H-15/H-16/H-17. The presence of epoxy group located at C-14 (δ_C 71.1)/C-15 (δ_C 59.4) was determined to satisfy the one remaining degree of unsaturation in conjuction with the MS data. Thus, a preurianin-type limonoid matches with the main skeleton in compound **2**. The remaining signals and observed correlations, including H-2' (δ_H 1.89)/H-12 (δ_H 5.81) to C-1' (δ_C 175.0) and H-2" (δ_H 2.08)/H-11 (δ_H 5.60) to C-1" (δ_C 170.4), established the substitution of 2-methylbutoyloxy and ecetoxy at C-12 and C-11, respectively (**Figure 3**).

A NOESY experiment was consequently performed to deduce the relative configuration in **2** (**Figure 4**). Notable cross-peaks were observed between H-5/α and H-9/H_3-28, as well as between H-9 and H-11, indicating a co-facial relationship among these protons. In contrast, H_3-29 and the acyloxy group at C-11 are positioned oppositely. The single bond linking C-9 and C-10, along with the surrounding structures, is notably congested, which may lead to stereochemical complications. A comparison of NMR data for compound **2** with existing literature on preurianin and related compounds has established the orientation of H-5 and H-9 as proton-α, supported by NMR analysis conducted at non-ambient temperatures and X-ray diffraction studies (Vincent et al., 1975). Additionally, the correlation between H-12 and H-17, as well as H-11 and H_3-18, suggested that these proton pairs are situated on the same side, with H-12/H-17 exhibiting a β orientation and H-11/H_3-18 displaying an α orientation, thereby confirming a 1,2-diaxial relationship between H-11/H-12. As a result, the 2-methylbutanoyloxy group located at C-12 and the furan ring at C-17 are positioned towards the α side, while the acyloxy group at C-12 is directed towards the β side. The β orientation of the 14,15-epoxide was established through the correlation of H_3-18/α with H-30a, H-30a with H-15 (Govindachari et al., 1999; Maclachlan & Taylor, 1982). Further comparison of 1D-NMR data of **2** with amotsangin A reported from the same family Meliaceae, showed that they have identical chemical shifts (**Table 2**) (Chen et al., 2008). Hence, the structure of **2** was then identified and designated as amotsangin A, shown in Fig. 2. It is important to note that amotasangin A (**2**), a highly oxidized *seco*-limonoid compound, , is reported for the first time from the genus *Dysoxylum*, specifically from *D. parasiticum*. Although structurally related limonoids have previously been identified within the Meliaceae family, including other *Dysoxylum* species (Naini et al., 2024b), this discovery broadens the known structural diversity of secondary metabolites in *D. parasiticum* and enriches the phytochemical profile of the genus *Dysoxylum*.

22(*E*)-ergosta-6,22-dien-3β,5α,8α-triol (**3**), was obtained as a white powder. The molecular formula was established as $C_{28}H_{46}O_3$ by its HR-QTOFMS/ESI$^+$, *m/z* 453.3351 (calculated for. *m/z* 453.3345, [M + Na]$^+$), referencing to six unsaturated degrees. The ^{1}H-NMR data of **3** showed six methyl resonances, involving two tertiary groups [δ_H 0.87 (3H, s) and 0.89 (3H, *s*) ppm] and four secondary methyls [δ_H 0. 81 (3H, d, J = 6.5 Hz), 0. 84 (3H, d, J = 6.5 Hz), 0. 93 (3H, d, J = 6.1 Hz), 1.01 (3H, d, J = 6.5 Hz) ppm]. Similar to those of isolated compounds **1** and **2**, the structure elucidation of **3** was therefore supplemented by ^{13}C-NMR and DEPT experiments, generating 28 carbon resonances. The two non-oxygenated quaternary carbons (δ_C 37.0 and 44.6 ppm) aligned with the existance of two tertiray methyls, as well as four secondary methyl groups (CH_3-21, CH_3-26, CH_3-27, and CH_3-28) located in the side chain, indicated that compound **3** is an ergostane-type steroid. An ergostane-type steroid is characterized by the presence of an extra secondary methyl group [δ_C 20.9 (δ_H 1.01, d, 6.5 Hz)] at the C-24 position, in addition to a notable double bond of -CH=CH- found between C-22 [δ_C 132.2 (δ_H 5.18, m) ppm] and C-23, [δ_C 135.7 (δ_H 5.22, m) ppm]. Moreover, the existance of a second paired olefinic bond characterized by the -CH=CH- fragment at [δ_C 135.4 (δ_H 6.60, m) and 130.7 (δ_H 6.33, m) ppm] was attributed to the C-6/C-7 system, similar to other ergostane-type steroids derived from the Meliaceae family. The presence of hydroxyl methine resonances at δ_C 66.5 (δ_H 3.95, m) was inferred to be located at C-3, based on the biogenetic perspective of steroids derived from 2,3-epoxy squalene. The two remaining oxygenated nonprotonated carbon groups observed at δ_C 82.2 and 79.4 ppm were assigned to C-5 and C-8, respectively, contributing to the formation of a diol group. This assignment is supported by the mass spectrum data and the characteristics of related

Table 2. NMR data (^{1}H and ^{13}C-NMR, $CDCl_3$) of **2** with literature (^{13}C-NMR, $CDCl_3$)

No.	Compound **2** ($CDCl_3$)		Amotsangin A ($CDCl_3$) (Chen et al., 2008)
	^{1}H NMR (ΣH, mult., *J* Hz)	^{13}C NMR (mult.)	^{13}C NMR (mult.)
1.	6.89 (1H, *d*, 13.0)	148.5 (d)	148.5 (d)
2.	6.22 (1H, *d*, 13.1)	122.0 (d)	122.0 (d)
3.	-	166.5 (s)	166.5 (s)
4.	-	83.5 (s)	83.5 (s)
5.	3.25 (1H, *d*, 9.0)	50.1 (d)	50.0 (d)
6a	2.14 (1H, *dd*, 16.5; 9.2)	35.0 (t)	34.9 (d)
6b.	2.24 (1H, *d*, 16.6)		
7.	-	173.5 (s)	173.5 (s)
8.	-	136.9 (s)	136.7 (s)
9.	3.02 (1H, *d*, 7.2)	53.4 (d)	53.2 (d)
10.	-	46.2 (s)	46.2 (s)
11.	5.60 (1H, *dd*, 10.9; 7.1)	71.0 (d)	70.9 (d)
12.	5.81 (1H, *d*, 10.9)	73.6 (d)	73.6 (d)
13.	-	45.6 (s)	45.5 (s)
14.	-	71.1 (s)	71.0 (s)
15.	3.88 (1H, *s*)	59.6 (d)	59.0 (d)
16.	2.24 (1H, *dd*, 14.0, 7.0)	34.1 (t)	34.0 (t)
	1.83 (1H, *dd*, 14.0)		
17.	0.93 (3H, *s*)	42.7 (d)	37.6 (d)
18.	0.97 (3H, *s*)	13.6 (q)	13.6 (q)
19.	-	22.7 (q)	22.7 (q)
20.	7.07 (1H, *s*)	122.0 (s)	122.1 (s)
21.	6.16 (1H, *s*)	140.6 (d)	140.5 (d)
22.	7.25 (1H, *s*)	111.2 (d)	111.3 (d)
23.	1.25 (3H, *s*)	142.3 (d)	142.3 (d)
28.	1.52 (3H, *s*)	30.3 (q)	30.2 (q)
29.	5.17 (1H, *s*)	22.4 (q)	22.3 (q)
30a	5.34 (1H, *s*)	120.8 (t)	120.8 (t)
30b.	3.68 (3H, *s*)		
OMe.	-	52.3 (q)	52.3 (q)
1′.	1.89 (2H, *m*)	175.0 (s)	175.0 (s)
2′.	1.17 (1H, *m*)	40.5 (t)	41.1 (t)
3a′.	1.41 (1H, *m*)	25.7 (t)	25.9 (t)
3b′.	0.73 (3H, *t*, 7.3)		
4′.	0.79 (3H, *d*, 8.4)	11.4 (q)	11.7 (q)
5′.	-	15.2 (q)	15.3 (q)
1″.	2.08 (3H, *s*)	170.4 (s)	170.4 (s)
2″.	-	20.7 (q)	20.6 (q)

ergostane compounds that exhibit significant oxidation at these carbon positions. The determination of the structure for compound **3** was achieved through a limited set of experiments; however, the analysis of the resonances observed in the ^{1}H and ^{13}C-NMR data was sufficiently reliable to enable the complete construction of its structure. A subsequent literature review indicated that the ^{1}D-NMR data for compound **3** exhibited significant similarities to 22-(*E*)-ergosta-6,22-dien-3*β*,5*α*,8*α*-triol (**Table 3**), which was derived from the ethanolic extract of *Letinus edodes* (Shiitake) (Rivera et al., 2009). To our knowledge, 22(*E*)-ergosta-6,22-dien-3*β*,5*α*,8*α*-triol (**3**) (**Figure 2**), a polyhydroxylated ergostane-type steroid, is reported for the first time from *D. parasiticum*. This discovery contributes to the phytochemical profile of *D. parasiticum* and enriches the diversity of its secondary metabolites, particularly within the steroid class.

Activity against Breast Cancer MCF-7

In order to evaluate the biological activity of three identified compounds, they were tested against the human breast cancer MCF-7. Recent findings published by the World Health Organization (2018) indicate that breast cancer cases in Indonesia have reached unprecedented levels, accompanied by the second-highest mortality rate. Concurrently, the issue of drug resistance in MCF-7 cancer cells persists. This phenomenon is attributed to the luminal A subtype of

breast cancer cells, such as MCF-7, which, accounting for approximately 70% of cases, exhibit the expression of alpha estrogen receptors (ER-α). These receptors contribute to resistance against several chemotherapy agents, including doxorubicin (Lovitt et al., 2018; Chekhun et al., 2006; Fang et al., 2014; Chen et al., 2010), paclitaxel (Zhang et al., 2015; Pavlíková et al., 2015; Armat et al., 2016), tamoxifen (Yao et al., 2020; To et al., 2022; Zhang et al., 2015), and cisplatin (Kobayashi et al., 2022; Ruiz-Silvestre et al., 2024; Chen et al., 2016). Therefore, the exploration of natural materials for compounds exhibiting cytotoxic effects on MCF-7 cells continues to represent a promising avenue for the development of anticancer agents characterized by enhanced chemosensitivity. As shown in **Table 4**, among all three compounds **1-3**, compounds **1** and **3** showed no activity with their IC_{50} values over 100 µM, while compound **2** displayed more inhibitory effect with its IC_{50} value of 34.5 µM than the reference drug cisplatin (IC_{50}, 53.0 µM). According to the previous results, compound **2** possessed a potent antiviral against tobacco mosaic virus (Yan et al., 2015), while its cytotoxicity is reported for the first time in this work, unless the analog, paraxyline A, with modest cytotoxicity against MCF-7 and HeLa cells (Naini et al., 2024b). These results are also consistent with those observed for **1**, which showed no inhibitory activity against human lung cancer A549 cells (Riyadi et al., 2024d), and **3**, which was inactive against MCF-7 and HeLa cells (Naini et al., 2024b). The presence of highly modified limonoids, characterized by an opening in the A and B rings and significant substitution by ester derivatives at position **2**, may be essential in the fight against human cancer cells, despite the variation in their primary skeletal structures. Regardless of they all have different main skeletons and the structure activity-relationship (SAR) could not be explored, the occurrence of highly modified limonoids with an opening in the A, B-rings and highly substituted by ester derivatives in **2** might be necessary against human cancer cells.

Table 3. NMR data (^{1}H and ^{13}C-NMR, $CDCl_3$) of **3** with literature (^{13}C-NMR, $CDCl_3$)

No.	Compound **3** ($CDCl_3$)		22(*E*)-ergosta-6.22-dien-3*β*,5*α*,8*α*-triol ($CDCl_3$) (Rivera et al., 2009)
	^{1}H NMR (ΣH, mult., *J* Hz)	^{13}C NMR (mult.)	^{13}C NMR (mult.)
1.	1.96 (1H, *m*) 1.69 (1H, *m*)	34.2 (t)	34.7 (t)
2.	1.99 (1H, *m*) 1.24 (1H, *m*)	39.3 (t)	39.3 (t)
3.	3.95 (1H, *m*)	66.5 (d)	66.5 (d)
4.	1.92 (2H, *m*)	36.9 (t)	36.9 (t)
5.	-	82.2 (s)	82.2 (s)
6.	6.60 (1H, *m*)	135.4 (d)	135.4 (d)
7.	6.33 (1H, *m*)	130.7 (d)	130.7 (d)
8.	-	79.4 (s)	79.4 (s)
9.	1.59 (1H, *m*)	51.7 (d)	51.7 (d)
10.	-	37.0 (s)	37.0 (s)
11.	1.62 (2H, *m*)	20.6 (t)	20.6 (t)
12.	1.52 (2H, *m*)	30.1 (t)	30.1 (t)
13.	-	44.6 (s)	44.6 (s)
14.	1.19 (1H, *m*)	55.9 (d)	56.2 (d)
15.	1.22 (2H, *m*)	22.9 (t)	23.4 (t)
16.	1.23 (2H, *m*)	28.6 (t)	28.6 (t)
17.	1.51 (1H, *m*)	33.1 (d)	33.1 (d)
18.	0.87 (3H, *s*)	12.9 (q)	12.9 (q)
19.	0.89 (3H, *s*)	18.2 (q)	18.2 (q)
20.	1.82 (1H, *m*)	42.8 (d)	42.8 (d)
21.	0.93 (3H, *d*, 6.4)	17.6 (q)	17.6 (q)
22.	5.18 (1H, *m*)	132.2 (d)	132.3 (d)
23.	5.22 (1H, *m*)	135.7 (d)	135.2 (d)
24.	2.02 (1H, *m*)	39.7 (d)	39.7 (d)
25.	1.85 (1H, *m*)	51.5 (d)	51.1 (d)
26.	0.84 (3H, *d*, 6.5)	19.9 (q)	19.9 (q)
27.	0.81 (3H, *d*, 6.5)	19.6 (q)	19.6 (q)
28.	1.01 (3H, *d*, 6.5)	20.9 (q)	20.9 (q)

Table 4. Cytotoxic activity of 1-3 against human cancer cell lines (IC_{50} ± SD, μM)[a]

Compounds	MCF-7
1	>100
2	34.5 ± 2.1
3	>100
Cisplatin[b]	53.0 ± 0.1

[a] Data were reported as the mean ± SD; n = 3 independent replicates
[b] Positive control

Among the three tested compounds, only amotsangin A (**2**) demonstrated notable cytotoxicity, with an IC_{50} value of 34.5 ± 2.1 μM, outperforming cisplatin. The superior activity of **2** can be attributed to its highly oxidized *seco*-limonoid framework, characterized by A and B ring cleavage and extensive ester substitutions. These structural features play a crucial role in enhancing cytotoxicity. Notably, amotsangin A is reported here for the first time from the genus *Dysoxylum*, specifically from *D. parasiticum*, adding a novel member to the chemical profile of this genus. In contrast, compounds **1** and **3** exhibited no significant activity (IC_{50} >100 μM), highlighting the importance of specific oxidation patterns and ring modifications in determining anticancer efficacy.

CONCLUSIONS

In this phytochemical investigation, we present the isolation and characterization of three known compounds derived from the stem barks of *Dysoxylum parasiticium*, specifically cneorin-NP36 (**1**), amotsangin A (**2**), and 22(*E*)-ergosta-6,22-dien-3*β*,5*α*,8*α*-triol (**3**). Compound **1** is identified as a triterpenoid characterized by a tirucallane-type backbone, notable for its paired double bond system located at C-7/C-8. It is differentiated from its stereoisomer, the euphane-type, by the *β*-orientation of the CH_3-21 group at C-20. Compound **2** is classified within the *seco*-limonoid category, specifically of the preurianin type, exhibiting significant modifications to its fundamental structure, including the presence of an *α*,*β*-unsaturated-ε-caprolactone moiety in ring A and an opening in the B-ring. The extensive oxidation observed in compound **2** is reflected not only in its primary skeleton but also in the presence of two ester substituents at C-11 and C-12. Additionally, compound **3** is characterized by the presence of polyhydroxy groups typical of an ergostane-type steroid at positions C-3, C-5, and C-8. The biological efficacy of three identified compounds (**1-3**) demonstrated that the modified limonoid in compound **2** exhibits superior inhibitory effects on the growth of the human breast cancer cell line MCF-7 compared to the established chemotherapeutic agent cisplatin (IC_{50}, 53.0 μM), with an IC_{50} value of 34.5 μM for the modified limonoid. According to Naini et al. (2024b), preurianin-type limonoids from *D. parasiticum,* such as paraxylines A–G, showed notable cytotoxic activity against MCF-7 and HeLa cancer cell lines, which was strongly associated with their high oxygenation levels and distinct ring modifications. In line with these findings, amotsangin A (**2**) also a highly oxygenated preurianin-type limonoid demonstrated potent cytotoxicity against MCF-7 cells.

ACKNOWLEDGEMENTS

This investigation was funded by Jambi University Under the Internal Grant, 2024 (HR)

REFERENCES

Armat, M., Bakhshaiesh, T. O., Sabzichi, M., Shanehbandi, D., Sharifi, S., Molavi, O., Mohammadian, J., Hejazi, M. S., & Samadi, N. (2016). The role of Six1 signaling in paclitaxel-dependent apoptosis in MCF-7 cell line. *Bosnian Journal of Basic Medical Sciences*, *16*(1), 28.

Ashwell, D., & Walston, N. (2008). An overview of the use and trade of plants and animals in traditional medicine systems in Cambodia. *A Traffic Southeast Asia Report*, 39–44.

Atkinson, B. A. (2020). Fossil evidence for a Cretaceous rise of the mahogany family. *American Journal of Botany*, *107*(1), 139–147.

Bourdy, G., Francois, C., Andary, C., & Boucard, M. (1996). Maternity and medicinal plants in Vanuatu II. Pharmacological screening of five selected species. *Journal of Ethnopharmacology, 52*(3), 139–143.

Chanda, R., Mohanty, J., Bhuyan, N., Kar, P., & Nath, L. (2007). Medicinal pants used against gastrointestinal tract disorders by the traditional healers of Sikkim Himalayas. *Indian Journal of Traditional Knowledge, 6*(4), 606–610.

Chekhun, V. F., Kulik, G. I., Yurchenko, O. V., Tryndyak, V. P., Todor, I. N., Luniv, L. S., Tregubova, N. A., Pryzimirska, T. V., Montgomery, B., Rusetskaya, N. V., & Pogribny, I. P. (2006). Role of DNA hypomethylation in the development of the resistance to doxorubicin in human MCF-7 breast adenocarcinoma cells. *Cancer Letters, 231*(1), 87–93.

Chen, G. Q., Zhao, Z. W., Zhou, H. Y., Liu, Y. J., & Yang, H. J. (2010). Systematic analysis of microRNA involved in resistance of the MCF-7

human breast cancer cell to doxorubicin. *Medical Oncology, 27*, 406–415.

Chen, H. D., Yang, S. P., Liao, S. G., Zhang, B., Wu, Y., & Yue, J. M. (2008). Limonoids and sesquiterpenoids from *Amoora tsangii*. *Journal of Natural Products, 71*(1), 93–97.

Chen, X., Lu, P., Wu, Y., Wang, D. D., Zhou, S., Yang, S. J., Shen, H. Y., Zhang, X. H., Zhao, J. H., & Tang, J. H. (2016). MiRNAs-mediated cisplatin resistance in breast cancer. *Tumor Biology, 37*, 12905–12913.

Fang, X. J., Jiang, H., Zhu, Y. Q., Zhang, L. Y., Fan, Q. H., & Tian, Y. (2014). Doxorubicin induces drug resistance and expression of the novel CD44st via NF-κB in human breast cancer MCF-7 cells. *Oncology Reports, 31*(6), 2735–2742.

Govindachari, T. R., Suresh, G., Kumari, G. N. K., Rajamannar, T., & Partho, P. D. (1999). Nymania-3: A bioactive triterpenoid from *Dysoxylum malabaricum*. *Fitoterapia, 70*(1), 83–86.

Gray, A. I., Bhandarit, P., & Waterman, P. G. (1988). New protolimonoids from the fruits of *Phellodendron chinense*. *Phytochemistry, 27*(6), 1805–1808.

Hill, R. A., & Connolly, J. D. (2017). Triterpenoids. *Natural Product Reports, 34*(1), 90–122.

Hu, J., Song, Y., Li, H., Yang, B., Mao, X., Zhao, Y., & Shi, X. (2014). Cytotoxic and anti-inflammatory tirucallane triterpenoids from *Dysoxylum binectariferum*. *Fitoterapia, 99*, 86–91.

Huang, H. L., Wang, C. M., Wang, Z. H., Yao, M. J., Han, G. T., Yuan, J. C., Gao, K., & Yuan, C. S. (2011). Tirucallane-type triterpenoids from *Dysoxylum lenticellatum*. *Journal of Natural Products, 74*(10), 2235–2242.

Jian, L. C., Kernan, M. R., Jolad, S. D., Stoddart, C. A., Bogan, M., & Cooper, R. (2007). Dysoxylins A–D, tetranortriterpenoids with potent anti-RSV activity from *Dysoxylum gaudichaudianum*. *Journal of Natural Products, 70*(2), 312–315.

Jogia, M. K., & Andersen, R. J. (1987). Dysoxylin, a limonoid from *Dysoxylum richii*. *Phytochemistry, 26*(12), 3309–3311.

Kautsari, A., Naini, A. A., Mayanti, T., Nurlelasari, N., Harneti, D., Farabi, K., Maharani, R., Harizon, H., Nurul Azmi, M. N., & Supratman, U. (2024a). Excelxylin A: A new seco A-ring tirucallane triterpenoid from the stem bark of *Dysoxylum excelsum*. *Journal of Asian Natural Products Research, 26*(7), 843–849.

Kautsari, A., Naini, A. A., Riyadi, S. A., Mayanti, T., Harizon, H., Fajriah, S., & Supratman, U. (2024b). Sesquiterpenoids from the stem bark of *Dysoxylum excelsum* and their cytotoxic activities against HeLa cancer cell lines. *Molekul, 19*(1), 109–116.

Kobayashi, M., Yonezawa, A., Takasawa, H., Nagao, Y., Iguchi, K., Endo, S., Ikari, A., & Matsunaga, T. (2022). Development of cisplatin resistance in breast cancer MCF7 cells by up-regulating aldo-keto reductase 1C3 expression, glutathione synthesis and proteasomal proteolysis. *Journal of Biochemistry, 171*(1), 97–108.

Kumar, V., Guru, S. K., Jain, S. K., Joshi, P., Gandhi, S. G., Bharate, S. B., Bhushan, S., Bharate, S. S., & Vishwakarma, R. A. (2016). A chromatography-free isolation of rohitukine from leaves of *Dysoxylum binectariferum*: Evaluation for in vitro cytotoxicity, Cdk inhibition and physicochemical properties. *Bioorganic & Medicinal Chemistry Letters, 26*(15), 3457–3463.

Lakshmi, V., Pandey, K., & Agarwal, S. K. (2009). Bioactivity of the compounds in genus *Dysoxylum*. *Acta Ecologica Sinica, 29*(1), 30–44.

Lalmuanpuii, J., Rosangkima, G., & Lamin, H. (2013). Ethno-medicinal practices among the Mizo ethnic group in Lunglei district, Mizoram. *Science Vision, 13*(1), 24–34.

Liu, H., Heilmann, J., Rali, T., & Sticher, O. (2001). New tirucallane-type triterpenes from *Dysoxylum variabile*. *Journal of Natural Products, 64*(2), 159–163.

Lovitt, C. J., Shelper, T. B., & Avery, V. M. (2018). Doxorubicin resistance in breast cancer cells is mediated by extracellular matrix proteins. *BMC Cancer, 18*(1), 1–11.

Maclachlan, L. K., & Taylor, D. A. H. (1982). Limonoids from *Nymania capensis*. *Phytochemistry, 21*(7), 1701–1703.

Nagakura, Y., Yamanaka, R., Hirasawa, Y., Hosoya, T., Rahman, A., Kusumawati, I., Zaini, N. C., & Morita, H. (2010). Gaudichaudysolin A, a new limonoid from the bark of *Dysoxylum gaudichaudianum*. *Heterocycles, 80*(2), 1471–1477.

Naini, A. A., Mayanti, T., Darwati, -, Harneti, D., Nurlelasari, N., Maharani, R., Farabi, K., Herlina, T., Supratman, U., Fajriah, S., Kuncoro, H., Azmi, M. N., Shiono, Y., Jungsuttiwong, S., & Chakthong, S. (2023a). Sesquiterpenoids and sesquiterpenoid dimers from the stem bark of *Dysoxylum parasiticum* (Osbeck) Kosterm. *Phytochemistry, 205*, 113477.

Naini, A. A., Mayanti, T., Hilmayanti, E., Huang, X., Kabayama, K., Shimoyama, A., Manabe, Y., Fukase, K., & Supratman, U. (2024a). Immunomodulatory of sesquiterpenoids and sesquiterpenoid dimers-based toll-like receptor 4 (TLR4) from *Dysoxylum parasiticum* stem bark. *Scientific Reports, 14*(1), 15597.

Naini, A. A., Mayanti, T., Maharani, R., Fajriah, S., Kabayama, K., Shimoyama, A., Manabe, Y., Fukase, K., Jungsuttiwong, S., & Supratman, U. (2023b). Dysoticans F–H: Three unprecedented dimeric cadinanes from *Dysoxylum parasiticum* (Osbeck) Kosterm. stem bark. *RSC Advances, 13*(14), 9370–9376.

Naini, A. A., Mayanti, T., Maharani, R., Harneti, D., Nurlelasari, N., Farabi, K., Fajriah, S., Hilmayanti, E., Kabayama, K., Shimoyama, A., Manabe, Y., Fukase, K., Jungsuttiwong, S., Prescott, T. A. K., & Supratman, U. (2024b). Paraxylines A–G: Highly oxygenated preurianin-type limonoids with immunomodulatory TLR4 and cytotoxic activities from the stem bark of *Dysoxylum parasiticum*. *Phytochemistry, 220*, 114009.

Naini, A. A., Mayanti, T., Nurlelasari, N., Harneti, D., Maharani, R., Safari, A., Hidayat, A. T., Farabi, K., Lesmana, R., Supratman, U., & Shiono, Y. (2022a). Cytotoxic sesquiterpenoids from *Dysoxylum parasiticum* (Osbeck) Kosterm. stem bark. *Phytochemistry Letters, 47*, 102–106.

Naini, A. A., Mayanti, T., & Supratman, U. (2022b). Triterpenoids from *Dysoxylum* genus and their biological activities. *Archives of Pharmacal Research, 45*(2), 63–89.

Pavlíková, N., Bartoňová, I., Balušíková, K., Kopperova, D., Halada, P., & Kovář, J. (2015). Differentially expressed proteins in human MCF-7 breast cancer cells sensitive and resistant to paclitaxel. *Experimental Cell Research, 333*(1), 1–10.

Rivera, A., Benavides, O. L., & Rios-Motta, J. (2009). (22E)-Ergosta-6,22-diene-3β5α8α-triol: A new polyhydroxysterol isolated from *Lentinus edodes* (Shiitake). *Natural Product Research, 23*(3), 293–300.

Riyadi, S. A., Naini, A. A., Mayanti, T., Farabi, K., Harneti, D., Nurlelasari, N., Maharani, R., Lesmana, R., Fajriah, S., Jungsuttiwong, S., Awang, K. B., Nurul Azmi, M. N., & Supratman, U. (2024a). Alliaceumolide A: A rare undescribed 17-membered macrolide from Indonesian *Dysoxylum alliaceum*. *Phytochemistry Letters, 62*, 73–77.

Riyadi, S. A., Naini, A. A., Mayanti, T., Farabi, K., Lesmana, R., Nurul Azmi, M. N., Fajriah, S., & Supratman, U. (2024b). Cytotoxic tirucallanes from *Dysoxylum alliaceum* stem barks in human cancer and normal cells lines. *Journal of Biological Active Products from Nature, 14*(2), 171–186.

Riyadi, S. A., Naini, A. A., Mayanti, T., Lesmana, R., Nurul Azmi, M. N., Fajriah, S., Jungsuttiwong, S., & Supratman, U. (2024c). Alliaxylines A–E: Five new mexicanolides from the stem barks of *Dysoxylum alliaceum* (Blume) Blume ex A. Juss. *Journal of Natural Medicines, 78*(3), 558–567.

Riyadi, S.A., Naini, A.A., Mayanti, T., Lesmana, R., Azmi, M.N. and Supratman, U. (2024d). The Cytotoxic Evaluation of Steroids Isolated from *Dysoxylum alliaceum* (Blume) Blume ex A. Juss. *Molekul*, *19*(3), pp.471-480.

Ruiz-Silvestre, A., Garcia-Venzor, A., Ceballos-Cancino, G., Sánchez-López, J. M., Vazquez-Santillan, K., Mendoza-Almanza, G., Lizarraga, F., Melendez-Zajgla, J., & Maldonado, V. (2024). Transcriptomic changes in cisplatin-resistant MCF-7 cells. *International Journal of Molecular Sciences, 25*(7), 3820.

Sarkar, M., & Devi, A. (2017). Analysis of medicinal and economic important plant species of Hollongapar Gibbon wildlife sanctuary, Assam, northeast India. *Tropical Plant Research, 4*(3), 486–495.

Sawai, S., & Saito, K. (2011). Triterpenoid biosynthesis and engineering in plants. *Frontiers in Plant Science, 2*(25), 1–8.

Singh, Y., & Aalbersberg, W. (1992). Dammarane triterpenoids from *Dysoxylum richii*. *Phytochemistry, 31*(11), 921–926.

Sofian, F. F., Subarnas, A., Hakozaki, M., Uesugi, S., Koseki, T., & Shiono, Y. (2022). Bidysoxyphenols A–C, dimeric sesquiterpene phenols from the leaves of *Dysoxylum parasiticum* (Osbeck) Kosterm. *Fitoterapia, 158*, 105157.

Sofian, F. F., Subarnas, A., Hakozaki, M., Uesugi, S., Koseki, T., & Shiono, Y. (2022). Tridysoxyphenols A and B, two new trimeric sesquiterpene phenols from *Dysoxylum parasiticum* leaves. *Phytochemistry Letters, 50*, 134–140.

Tan, Q. G., & Luo, X. D. (2011). Meliaceous limonoids: Chemistry and biological activities. *Chemical Reviews, 111*(11), 7437–7522.

To, N. B., Truong, V. N. P., Ediriweera, M. K., & Cho, S. K. (2022). Effects of combined pentadecanoic acid and tamoxifen treatment on tamoxifen resistance in MCF−7/SC breast cancer cells. *International Journal of Molecular Sciences, 23*(19), 11340.

Vincent Gullo, B. P., Miura, I., Nakanishi, K., Forbes Cameron, A., Connolly, J. D., Duncanson, F. D., Harding, A. E., McCrindle, R., & Taylor, D. A. H. (1975). Structure of prieurianin, a complex tetranortriterpenoid; nuclear magnetic resonance analysis at nonambient temperatures and X-ray structure determination. *Journal of the Chemical Society, Chemical Communications, 9*, 345–346.

Wang, F., & Guan, Y. (2012). Cytotoxic nor-dammarane triterpenoids from *Dysoxylum hainanense*. *Fitoterapia, 83*(1), 13–17.

Wang, J. R., Liu, H. L., Kurtán, T., Mándi, A., Antus, S., Li, J., Zhang, H. Y., & Guo, Y. W. (2011). Protolimonoids and norlimonoids from the stem

bark of *Toona ciliata* var. *pubescens*. *Organic & Biomolecular Chemistry, 9*(22), 7685–7696.

Xu, J., Ni, G., Yang, S., & Yue, J. (2013). Dysoxylumasins A–F: Six new limonoids from *Dysoxylum mollissimum* Bl. *Chinese Journal of Chemistry, 31*(1), 72–78.

Yan, Y., Yuan, C.M., Di, Y.T., Huang, T., Fan, Y.M., Ma, Y., Zhang, J.X. and Hao, X.J. (2015). Limonoids from *Munronia henryi* and their anti-tobacco mosaic virus activity. *Fitoterapia*, *107*, pp.29-35.

Yan, H. J., Si, H. L., Zhao, H. W., Chen, L., Yu, J. Q., Zhao, H. Q., & Wang, X. (2021). Four new cycloartane triterpenoids from the leaves of *Dysoxylum binectariferum*. *Phytochemistry Letters, 41*, 101–105.

Yao, J., Deng, K., Huang, J., Zeng, R., & Zuo, J. (2020). Progress in the understanding of the mechanism of tamoxifen resistance in breast cancer. *Frontiers in Pharmacology, 9*(11), 592912.

Zhang, W., Cai, J., Chen, S., Zheng, X., Hu, S., Dong, W., Lu, J., Xing, J., & Dong, Y. (2015). Paclitaxel resistance in MCF-7/PTX cells is reversed by paeonol through suppression of the SET/phosphatidylinositol 3-kinase/Akt pathway. *Molecular Medicine Reports, 12*(1), 1506–1514.

Zhang, X., Zhang, B., Liu, J., Liu, J., Li, C., Dong, W., Fang, S., Li, M., Song, B., Tang, B., & Wang, Z. (2015). Mechanisms of gefitinib-mediated reversal of tamoxifen resistance in MCF-7 breast cancer cells by inducing ERα re-expression. *Scientific Reports, 5*(1), 7835.

Zhang, X. Y., Li, Y., Wang, Y. Y., Cai, X. H., Feng, T., & Luo, X. D. (2010). Tirucallane-type alkaloids from the bark of *Dysoxylum laxiracemosum*. *Journal of Natural Products, 73*(8), 1385–1388.

Zuo, K., Zhang, X. P., Zou, J., Li, D., & Lv, Z. W. (2010). Establishment of a paclitaxel resistant human breast cancer cell strain (MCF-7/Taxol) and intracellular paclitaxel binding protein analysis. *Journal of International Medical Research, 38*(4), 1428–1435.